Published in final edited form as:
Plant J. 2009 January ; 57(2): 332–345. doi:10.1111/j.1365-313X.2008.03693.x.

The BTB ubiquitin ligases ETO1, EOL1 and EOL2 act collectively to regulate ethylene biosynthesis in Arabidopsis by controlling type-2 ACC synthase levels

Matthew J. Christians[1,†], **Derek J. Gingerich**[1,‡,†], **Maureen Hansen**[3,†], **Brad M. Binder**[2,§], **Joseph J. Kieber**[3], and **Richard D. Vierstra**[1,*]

[1]Department of Genetics, 425-G Henry Mall, University of Wisconsin Madison WI 53706−1574, USA

[2]Department of Horticulture, 1575 Linden Drive, University of Wisconsin Madison WI 53706−1574, USA

[3]Department of Biology, Coker Hall, University of North Carolina Chapel Hill, NC 27599−3280, USA

Summary

Ethylene biosynthesis is directed by a family of 1-aminocyclopropane-1-carboxylic acid (ACC) synthases (ACS) that convert *S*-adenosyl-L-methionine to the immediate precursor ACC. Members of the type-2 ACS subfamily are strongly regulated by proteolysis with various signals stabilizing the proteins to increase ethylene production. In Arabidopsis, this turnover is mediated by the ubiquitin/26 S proteasome system, using a broad complex/tramtrack/bric-a-brac (BTB) E3 assembled with the ETHYLENE OVERPRODUCER 1 (ETO1) BTB protein for target recognition. Here, we show that two Arabidopsis BTB proteins closely related to ETO1, designated ETO1-like (EOL1) and EOL2, also negatively regulate ethylene synthesis via their ability to target ACSs for breakdown. Like ETO1, EOL1 interacts with type-2 ACSs (ACS4, ACS5 and ACS9), but not with type-1 or type-3 ACSs, or with type-2 ACS mutants that stabilize the corresponding proteins *in planta*. Whereas single and double mutants affecting *EOL1* and *EOL2* do not show an ethylene-related phenotype, they exaggerate the effects caused by inactivation of *ETO1*, and further increase ethylene production and the accumulation of ACS5 in *eto1* plants. The triple *eto1 eol1 eol2* mutant phenotype can be effectively rescued by the ACS inhibitor aminoethoxyvinylglycine, and by silver, which antagonizes ethylene perception. Together with hypocotyl growth assays showing that the sensitivity and response kinetics to ethylene are normal, it appears that ethylene synthesis, but not signaling, is compromised in the triple mutant. Collectively, the data indicate that the Arabidopsis BTB E3s assembled with ETO1, EOL1 and EOL2 work together to negatively regulate ethylene synthesis by directing the degradation of type-2 ACS proteins.

Keywords

ubiquitin; ethylene; 1-aminocyclopropane-1-carboxylic acid; protein degradation

*For Correspondence (fax 608 262 2976; e-mail vierstra@wisc.edu)..
†All three authors contributed equally to this work.
‡Present address: Department of Biology, University of Wisconsin-Eau Claire, Eau Claire, WI.
§Present address: Department of Biochemistry and Cellular and Molecular Biology, University of Tennessee, Knoxville, TN.

Introduction

Ethylene is an important gaseous hormone that regulates numerous aspects of plant growth and development. Under normal conditions, it controls hypocotyl and root elongation, apical hook formation, root hair development, leaf and flower senescence/abscission, stem cell division in roots and fruit ripening (Abeles *et al*., 1992; Johnson and Ecker, 1998; Schaller and Kieber, 2002; Ortega-Martinez *et al*., 2007). Through its ability to readily permeate through cell membranes, ethylene also provides a mechanism for plants to rapidly and coordinately respond to adverse environments, such as pathogen attack, wounding, hypoxia, and exposure to drought and cold. Consequently, both the synthesis and perception of ethylene are tightly controlled within plants.

Extensive genetic analyses with Arabidopsis have uncovered elaborate pathways that mediate both ethylene synthesis and perception (Argueso *et al*., 2007; Benavente and Alonso, 2006). Ethylene perception employs an inverse agonist mechanism that begins with a family of five receptors related to bacterial two-component histidine kinases. In the absence of ethylene, they activate CONSTITUTIVE TRIPLE RESPONSE-1 (CTR1), a Raf-type mitogen-activated protein kinase kinase kinase (MAPKKK) that inhibits ethylene signaling (Chang *et al*., 1993; Hirayama *et al*., 1999; Hua *et al*., 1995, 1998; Kieber *et al*., 1993). Binding of ethylene blocks this activation of CTR1, thus allowing ethylene signaling to commence towards ETHYLENE INSENSITIVE (EIN)-2. EIN2 is a membrane-associated positive regulator related to the N-ramp family of divalent cation transporters (Alonso *et al*., 1999), the action of which remains unclear. It interacts with a putative CONSTITUTIVELY PHOTOMORPHOGENIC (COP)-9 signalosome component (at least in yeast) that may modulate its activity (Christians *et al*., 2008). Ultimately, the pathway converges towards the transcription factors EIN3 and EIN3-LIKE (EIL)-1 that induce the expression of various ethylene-regulated genes, including *ERF1*, which encodes a key ethylene-response transcription factor (Chao *et al*., 1997; Yanagisawa *et al*., 2003). Both the EIN3 and EIL1 proteins are continually synthesized; however, in the absence of ethylene they are rapidly degraded to prevent ethylene responses. This turnover is accomplished by the ubiquitin (Ub)/26 S proteasome system (UPS), using a pair of Skp/Cullin/F-Box (SCF) E3s assembled with the EIN3-BINDING F-BOX (EBF)-1 and EBF2 F-box proteins that coordinately ubiquitinate EIN3/EIL1 (Binder *et al*., 2007; Gagne *et al*., 2004; Guo and Ecker, 2003; Potuschak *et al*., 2003). Ethylene blocks this breakdown, possibly by the activation of a MAPK cascade containing MPKK9 and MPK6 that phosphorylates EIN3/EIL1, thus protecting EIN3/EIL1 from $SCF^{EBF1/2}$ recognition (Yoo *et al*., 2008). In this way, ethylene induces the rapid accumulation of EIN3/EIL1 to promote the transcription of ethylene response genes.

In a similar fashion, ethylene production is also tightly controlled using protein degradation as a key regulatory mechanism. The first committed and generally rate-limiting step of ethylene biosynthesis involves the conversion of *S*-adenosyl-L-methionine to the immediate ethylene precursor 1-aminocyclopropane-1-carboxylic acid (ACC) by a family of ACC synthases (ACSs) (Schaller and Kieber, 2002). Conversion of ACC to ethylene is then catalyzed by members of the ACC oxidase (ACO) family (Argueso *et al*., 2007). Consistent with their importance to ethylene production, multiple forms of both ACSs and ACOs are synthesized with unique expression patterns, and post-transcriptional controls. For example, eight and 10 loci express catalytically active ACS proteins in Arabidopsis and tomato, respectively, and each has distinct transcriptional profiles in response to cell/tissue type, developmental state and hormone treatments (Liang *et al*., 1995; Tsuchisaka and Theologis, 2004; Wang *et al*., 2005; Yamagami *et al*., 2003).

Members of the ACS family have been further categorized into three types (types-1, −2 and −3) based on the presence of distinct consensus sequences near their C termini (Yoshida *et*

al., 2005). For the type-1 and type-2 ACSs, it is now apparent that these C-terminal sequences mediate the stability of the corresponding isoforms. For example, the signature C-terminal extensions in type-1 ACSs from Arabidopsis (ACS1, ACS2 and ACS6) are phosphorylated by the MAPK MPK6, and possibly by a calcium-dependent protein kinase (CDPK) (Hernandez Sebastia *et al*., 2004; Liu and Zhang, 2004). This modification dramatically elevates type-1 ACS protein levels and ethylene production *in planta*, possibly by protecting the enzymes from the UPS. In support, a phosphomimic substitution of the phosphorylation site(s) in ACS6 acts as a gain-of-function mutant that elevates both ACS6 protein levels and ethylene synthesis (Joo *et al*., 2008). Similarly, dominant overproduction mutations, such as Arabidopsis *eto2* and *eto3*, were found to affect a conserved C-terminal extension in the type-2 ACSs, ACS5 and ACS9, respectively. These mutants dramatically increase ethylene production, not by increasing *ACS5* or *ACS9* transcription, but by stabilizing the encoded proteins. This stability is mediated in part by protecting the proteins from rapid breakdown by the UPS (Chae *et al*., 2003; Vogel *et al*., 1998; Wang *et al*., 2004; Woeste *et al*., 1999).

Details about how ACS protein levels are controlled mechanistically by the UPS are now emerging. Important progress was made recently for the type-2 clade from an analysis of a set of recessive mutants affecting the *ETHYLENE OVERPRODUCING-1* (*ETO1*) locus. The *eto1* mutants were isolated based on their constitutive ethylene response phenotype in the absence of exogenous ethylene, which could be rescued by treatment of mutant seedlings with the ethylene biosynthesis inhibitor aminoethoxyvinylglycine (AVG), suggesting that the encoded protein dampens ethylene production (Guzman and Ecker, 1990). Wang *et al*. (2004) subsequently discovered that the ETO1 protein is a member of the broad complex/tramtrack/bric-a-brac (BTB) protein superfamily that participates in substrate recognition via the UPS. BTB proteins assemble with the Cullin-3 isoform (CUL3a and CUL3b in Arabidopsis; Gingerich *et al*., 2005) and the Ub-conjugating enzyme (or E2) docking protein RBX1 to form Ub-protein ligases (or E3s) (Smalle and Vierstra, 2004). Specific protein–protein interaction motifs present in the BTB proteins confer selectivity towards their substrates. The observations that: (i) ETO1 interacts with CUL3a/b and type-2 ACSs such as ACS5; (ii) that this interaction requires the C-terminal extension of ACS5, known to be important for stability; and (iii) that *eto1* mutants have increased levels of ACS5 protein and increased ethylene production, whereas *ETO1* overexpression lines have decreased levels of ACS5 protein and decreased ethylene production, point to the BTB^{ETO1} complex directly participating in the ubiquitination and subsequent degradation of type-2 ACSs (Chae *et al*., 2003; Wang *et al*., 2004; Yoshida *et al*., 2005, 2006). Data showing that mutants affecting the overall activity of Cullin-based E3s also regulate ethylene synthesis, support this scenario (Bostick *et al*., 2004; Larsen and Cancel, 2004). However, the observation that ETO1 can inhibit the activity of recombinant ACS5 *in vitro* suggests that a direct effect on type-2 ACS activities is also possible (Wang *et al*., 2004).

Phylogenetic studies revealed that higher plants express a large collection of BTB proteins, with 80 and 149 members in Arabidopsis and rice, respectively (Gingerich *et al*., 2005, 2007). In particular, Arabidopsis contains two potential paralogs of ETO1, designated ETO1-LIKE 1 (EOL1) and EOL2, that share significant similarity to ETO1, including the presence of six tetratricopeptide repeats (TPR), and a coiled-coil motif at their C-terminal ends. With yeast two-hybrid (Y2H) screening we observed that EOL1 can also interact with ACS5, which suggests that these two BTB proteins also direct type-2 ACS ubiquitination and turnover (Wang *et al*., 2004; Yoshida *et al*., 2006). However, single homozygous-null mutants affecting *EOL1* and *EOL2* failed to display obvious growth defects, especially those related to ethylene overproduction, suggesting that EOL1 and EOL2 work outside of ethylene signaling, or have a more subtle effect on ethylene biosynthesis than ETO1 (Gingerich *et al*., 2005).

Here, we further explored the potential roles of EOL1 and EOL2 on ACS turnover and ethylene biosynthesis in Arabidopsis, via a comparative analysis of the ETO1/EOL1/EOL2 family. In agreement with its role in controlling type-2 ACSs, EOL1, like ETO1, interacts with type-2, but not type-1 and type-3, ACSs, or type-2 mutants that stabilize protein accumulation. Whereas single and double mutants affecting *EOL1* and *EOL2* do not show obvious ethylene-overproduction phenotypes, they do exaggerate the phenotype of etiolated seedlings defective in *ETO1*, and further increase ethylene production by *eto1* plants. The triple *eto1 eol1 eol2* mutant in particular displays a strong ethylene response phenotype, and substantially overproduces the hormone. Based on the accumulation of a Myc-tagged version of ACS5 in the mutant backgrounds, the exaggerated phenotypes of the double and triple mutants are directly caused by the effects of EOL1 and EOL2 on type-2 ACS protein levels. Collectively, the data indicate that the Arabidopsis BTB E3s assembled with ETO1, EOL1 and EOL2 work together to negatively regulate ethylene synthesis, by helping degrade type-2 ACSs.

Results

ETO1 and EOL1 specifically interact with type-2 ACSs

Sequence homology among ETO1, EOL1 and EOL2, including related TPR and coiled-coil regions, have strongly implicated EOL1 and EOL2 in the recognition and turnover of type-2 ACSs by the UPS (Gingerich *et al*., 2005; Wang *et al*., 2004). In fact, recent studies have shown that Arabidopsis EOL1, like ETO1, can interact with the type-2 ACS ACS5, and its potential ortholog LeACS3 from tomato, suggesting that the interactions between ETO1-like BTB proteins and type-2 ACSs are conserved among higher plants (Wang *et al*., 2004; Yoshida *et al*., 2005, 2006). To further support this scenario, we used Y2H screening to test the binding specificity of EOL1 with members of the type-1 (ACS2 and ACS6), type-2 (ASC4, ASC5 and ASC9) and type-3 (ACS7) ACS clades from Arabidopsis. (Examining EOL2 by our Y2H strategy was not possible because of its strong autoactivation in the bait activation domain vector; data not shown.) As shown in Figure 1, EOL1 has a similar binding specificity as ETO1. It interacted with all members of the type-2 clade, but not with members of the type-1 and type-3 ACS clades. In general, EOL1 induced higher β-galactosidase activity relative to ETO1 in the Y2H pairings, suggesting that EOL1 either binds type-2 ACSs better than ETO1, or is expressed at a higher level in yeast.

Prior genetic and interaction studies have implicated a conserved patch near the C terminus of type-2 ACSs (residues 453−469 in ACS5) as important for their interactions with ETO1 (Wang *et al*., 2004; Yoshida *et al*., 2005, 2006). We provided further support for this proposal by testing the interactions of ETO1 and EOL1 with ACS5 missing the last 78 amino acids ($ACS5^{\Delta}$), with ACS5 bearing the *eto2* mutation that alters the C⁻terminal 12 amino acids (Vogel *et al*., 1998), and with ACS9 bearing the *eto3* mutation, which replaces the conserved Val-457 with an aspartic acid residue (Chae *et al*., 2003). Prior studies showed that the *eto2* and *eto3* mutations increase ethylene synthesis, with the *eto2* mutation increasing the stability of the ASC5 protein (Chae *et al*., 2003). Here, the *eto2* mutation substantially impaired binding of ACS5 to both ETO1 and EOL1, whereas the *eto3* mutation impaired the binding of ACS9 to ETO1, but only modestly compromised the binding to EOL1 (Figure 1). The residual binding of $ACS5^{eto2}$ to ETO1 and EOL1, as compared with the cognate controls, was further reduced by removing the entire C-terminal region in the $ACS5^{\Delta}$ deletion (Figure 1).

It has been proposed that the CDPK-dependent phosphorylation of type-2 ACSs is a signal that interferes with ETO1 recognition, thus blocking the presumed ubiquitination and subsequent turnover of the enzymes (Hernandez Sebastia *et al.*, 2004). One possible CDPK site is present in the C-terminal extension of ACS5 at Ser-461. However, introduction of a phosphomimic aspartic acid residue at position 461 ($ACS5^{S461D}$), or its alanine control ($ACS5^{S461A}$) that cannot be phosphorylated (S461A) into ACS5, had no significant effect on binding to ETO1

or EOL1 (Figure 1), suggesting that modification of this residue by itself does not strongly modify the interaction of these proteins.

Identification of combinatorial mutants affecting ETO1, EOL1 *and* EOL2

To assess the roles of EOL1 and EOL2 *in planta*, we generated various combinations of the T-DNA insertion mutations *eto1−13*, *eol1−1* and *eol2−2*, previously described by Gingerich *et al*. (2005) in the Col-0 ecotype (Figure 2a). These insertions disrupt the respective coding regions, and block the detectable accumulation of the corresponding transcripts, strongly suggesting that they represent null alleles. To obtain each double mutant, the single *eto1−13*, *eol1−1* and *eol2−2* mutants were crossed in various combinations, and then the desired homozygous combinations were identified in F_2 populations. The triple homozygous mutant (*eto1−13 eol1−1 eol2−2*) was created from an *eol1−1 eol2−2* to *eol1−1 eto1−13* cross. As can be seen in Figure 2b, genotyping of two representative triple mutant individuals by genomic PCR with gene-specific and T-DNA left-border primers confirmed that these plants were homozygous for the three insertions.

When grown on soil under either long (16-h light/8-h dark) or short (8-h light/16-h dark) days, only plants harboring the *eto1−13* mutation were visibly affected (Figure 2c, d and data not shown). The single *eol1−1* and *eol2−2* mutants and the *eol1−1 eol2−2* double mutant were indistinguishable from the wild type, both as 4-week-old rosette plants and as 6-week-old plants with mature inflorescences. The homozygous *eto1−13 eol1−1* and *eto1−13 eol2−2* double mutants and the *eto1−13 eol1−1 eol2−2* triple mutant were morphologically similar to the *eto1−13* single mutant, including a compact rosette with smaller leaves, reduced petiole lengths and shorter inflorescences. Although slightly fewer seeds were produced in the various *eto1 −13* combinations, even the triple mutant was fertile, with no evidence of increased seed abortion (data not shown). Seed germination of the triple mutant also appeared to be robust. The *eto1−13* combinations were less affected than the constitutive ethylene signaling mutant *ctr1−1*, which has substantially decreased rosette size, darker color, reduced inflorescence height and compromised fertility (Figure 2c,d; Kieber *et al*., 1993). Taken together, it appears that ETO1 is mainly responsible for controlling type-2 ACS levels in light-grown plants, with EOL1 and EOL2 playing insignificant roles, at least under the growth conditions tested.

Ethylene responses of etiolated eto1, eol1 *and* eol2 *mutant seedlings*

Wild-type etiolated seedlings exposed to exogenous ethylene, or mutant seedlings that either overproduce ethylene or constitutively activate the ethylene response pathway, display a characteristic triple-response phenotype consisting of shorter, thicker hypocotyls, shorter roots with increased numbers of longer root hairs, and an exaggerated apical hook (Guzman and Ecker, 1990). This phenotype can be easily seen in 3-day-old etiolated *ctr1−1* and *eto1* seedlings (Figure 3; Kieber *et al*., 1993). Neither the *eol1−1* and *eol2−2* single mutants nor the *eol1−1 eol2−2* double mutant displayed even a mild form of the triple response, suggesting that both EOL1 and EOL2 contribute little to the ethylene response of etiolated plants. However, introgression of the *eol1−1* and *eol2−2* mutations into the *eto1−13* background appeared to accentuate the triple response of *eto1−13* seedlings, as quantified by hypocotyl elongation (Figure 3b), indicating that EOL1 and EOL2 have a detectable role that only becomes apparent in the absence of ETO1.

To confirm that the accentuated effect is related to ethylene synthesis, and not to ethylene perception or unrelated responses, we examined the response of the mutant combinations to the potent ethylene biosynthesis and perception inhibitors AVG and silver ($AgNO_3$), respectively. Silver locks the ethylene receptor in an active state that keeps CTR1 functional to repress signaling (Schaller and Kieber, 2002). Although silver is effective in wild-type seedlings, even high concentrations cannot block the constitutive signaling of the *ctr1−1*

mutant (Figure 3a, c; Kieber *et al*., 1993). When 3-day-old *eto1−13, eol1−1* and *eol2−2* mutant combinations were treated with silver, the triple response was mostly eliminated, indicating that ethylene responsiveness was normal, even for the triple mutant. The mutant combinations were also rescued phenotypically upon treatment with 10 μM AVG. In contrast to the short hypocotyls and exaggerated apical hooks of *ctr1−1* seedlings, the hypocotyl lengths and apical hooks of the double and triple mutant seedlings exposed to AVG were comparable with the wild type (Figure 3a, b). Taken together, it appears that the *eol1−1* and *eol2−2* mutations accentuate the triple response of *eto1−13* seedlings solely by increasing ethylene synthesis.

Based on the likely roles of ETO1, EOL1 and EOL2 in directing the turnover of type-2 ACSs, the higher-order mutant combinations assembled with *eto1−13, eol1−1* and *eol2−2* should have higher ACS activities than the *eto1−13* single mutant, and thus require higher AVG concentrations to rescue their triple-response defects. The AVG dose–response data in Figure 3b supports this notion. As an example, hypocotyl lengths of the *eto1−13* seedlings in 0.25 μM AVG were comparable with wild-type Col-0 (1.0 versus 1.1 cm), whereas the hypocotyl lengths of the *eto1−13 eol1−1* and *eto1−13 eol2−2* double mutants, and the *eto1−13 eol1−1 eol2−2* triple mutant, were only partially rescued (0.8, 0.7 and 0.4 cm, respectively). Even at the highest AVG concentration used (20 μM), several of the combinatorial mutants were shorter than the wild-type and single-mutant seedlings.

To further demonstrate that ethylene synthesis, and not perception, is affected upon elimination of ETO1, EOL1 and EOL2, we attempted to phenocopy the growth inhibition response of the mutants by exposing etiolated seedlings to ethylene or ACC. As shown in Figure 4a, wild-type seedlings, the *eol1−1* and *eol2−2* single mutants, and the *eol1−1 eol2−2* double mutant, became progressively shorter as the concentrations of ethylene or ACC increased. At saturating concentrations of each (100 μL L^{-1} and 10 μM, respectively), the hypocotyl lengths of all single, double and triple mutants were similar to that of *ctr1−1* seedlings in air. We also tested the response of the *eto1−13, eol1−1* and *eol2−2* mutant combinations to exogenous ethylene under growth conditions in which endogenous ethylene synthesis was inhibited by AVG (10 μM), to further confirm that ethylene perception was normal. The inhibition of hypocotyl growth of the mutants in response to 100 μL L^{-1} ethylene was nearly indistinguishable from each other, and from the wild type (data not shown).

The kinetics of ethylene perception were also similar for the triple mutant compared with the wild type and the *eto1−13* single mutant. As described by Binder *et al*. (2004a,b), using a time-lapsed imaging system, 3-day-old etiolated wild-type seedlings treated with 10 μM AVG respond rapidly to exogenous ethylene, with 10 μL L^{-1} inducing a detectable growth inhibition within 10 min (Figure 4b). The elongation rate reaches a transient plateau within 30 min (phase I), and then decreases further to an even lower elongation rate (phase II), which can be maintained for many hours by continuous ethylene exposure. Upon removal of ethylene, the elongation rate rapidly rises close to the pre-treatment rate, after a lag of approximately 30 min, followed by a dampening oscillation as the elongation rate re-equilibrates. A variety of mutants can substantially affect this response, including mutants in ethylene signaling components (*ein2* and *ein3*), and factors that that affect their stability (*ebf1, ebf2* and *ein5/xrn4*) (Binder *et al*., 2004a,b, 2007; Potuschak *et al*., 2006). *eto1−13* seedlings displayed similar growth kinetics to the wild type, indicating that removal of ETO1 does not perceptibly affect the various components of ethylene signaling (initiation, phase I, phase II and recovery) (Figure 4b). The *eto1−13 eol1−1 eol2−2* triple mutant also behaved similarly with indistinguishable onset times for initiation and recovery (Figure 4b). The only substantial differences were the magnitudes of the initial elongation rate before ethylene exposure, and the elongation rate recovery after ethylene removal. These differences presumably reflect the high levels of type-2 ACSs in the triple mutant background, which cannot be adequately blocked by AVG even with 10 μM concentrations (see Figure 3b).

Ethylene production is regulated by the entire ETO/EOL1/EOL2 gene family

Both the Y2H screening and growth assays with etiolated seedlings are consistent with EOL1 and EOL2 working in conjunction with ETO1 to direct the ubiquitination and subsequent degradation of type-2 ACSs, with ETO1 being the major contributor. Consequently, we predicted that the *eol1−1* and *eol2−2* mutations would enhance ethylene production when introduced into the *eto1−13* mutant background. To test this possibility, we measured ethylene production from etiolated seedlings harboring the various mutant combinations. Consistent with previous studies and our phenotypic data from etiolated and green plants, wild-type Col-0 seedlings produce little ethylene, whereas the *eto1−13* seedlings synthesized high levels of ethylene (Figure 5). The *eol1−1* and *eol2−2* single mutant seedlings, and the *eol1−1 eol2−2* double mutant seedlings, also released little ethylene. A slight but repeatable increase in emission over that seen from the wild type was detected for plants harboring the *eol2−2* mutation, suggesting that EOL2 contributes some to type-2 ACS turnover, even in the presence of ETO1. However, as suspected from the phenotypic data, a substantial increase in ethylene release was observed when the *eol2−2* mutation was added to *etol1−13*, and then when *eol1 −1* was added to the *eol2−2 eto1−13* double mutant (Figure 5). The triple mutant released the most ethylene, which was almost twice that of *eto1−13 eol2−2* and more than 140-fold higher than that of the wild type. The effect of EOL1 was observed only when both ETO1 and EOL2 were eliminated, suggesting that this BTB protein contributes the least to directing type-2 ACS proteins towards breakdown in etiolated seedlings.

ACS5 accumulation is affected by the entire ETO1/EOL1/EOL2 family

To confirm that the stability of type-2 ACS proteins is regulated, in part, by *EOL1* and *EOL2*, the steady-state levels of an epitope-tagged ACS5 protein were assessed in the single, double and triple mutants. The homozygous *eto1−13 eol1−1 eol2−2* line was crossed with a Col-0 line expressing an N-terminal 6X Myc-tagged ACS5 protein, under the control of a dexamethasone (Dex)-inducible promoter (Chae *et al*., 2003; JJK, unpublished data). Lines containing the *MYC-ACS5* transgene, together with the various combinations of the homozygous *eto1−13*, *eol1−1* and *eol2−2* mutations, were then isolated from a selfed F_2 population, and were tested for Myc-ACS5 protein accumulation with anti-Myc antibodies. In the absence of Dex, the expression of the *MYC-ACS5* transgene was not detected by semi-quantitative reverse-transcription (RT)-PCR of total seedling RNA, using a primer specific for the appended region encoding the Myc epitope, in combination with a primer within the *ACS5* coding region (Figure 6a). However, when grown on 12 nM Dex (a concentration sufficiently low to avoid saturating the expression of the *MYC-ACS5* transgene in the wild-type seedlings; Chae *et al*., 2003), relatively similar levels of expression (compared with the control *UBC21* transcript) were evident in all wild-type and mutant plants harboring the *MYC-ACS5* transgene (Figure 6a).

When crude extracts from Dex-treated seedlings were subjected to immunoblot analysis with anti-Myc antibodies, the Myc-ACS5 protein at the expected mass of approximately 62 kDa could also be detected in plants harboring the transgene (Figure 6b). Whereas the level of the Myc-ACS5 protein was low in wild-type plants, its levels were increased in all backgrounds harboring mutations in *ETO1*, *EOL1* and *EOL2*, either singly or in combinations. In accord with the ethylene synthesis measurements, the *eto1−13* mutation had the strongest effect on Myc-ACS5 levels, with the triple mutant and *eto1−13 eol2−2* double mutant containing the highest protein levels. However, whereas the effects of *eol1−1* and *eol2−2* mutations by themselves were not significant, with respect to ethylene synthesis, we could detect a small increase in Myc-ACS5 protein levels in the backgrounds containing the *eol1−1* and *eol2−2* mutations alone, or in combination (Figure 6b). These increases indicate that EOL1 and EOL2 can affect type-2 ACS protein levels, even in the presence of ETO1, but that these increases are not enough to substantially alter ethylene production.

Expression patterns of the ETO1/EOL1/EOL2 family

There are a number of possible reasons why ETO1, EOL1 and EOL2 might contribute differentially to ethylene synthesis, including the preference of each for specific members of the type-2 ACS family, different expression patterns for the corresponding genes and/or the possibility that each BTB protein accumulates to different levels. To examine the expression patterns, we assayed the abundance of each transcript by analysis of various transcriptome databases, RNA gel blot analysis and quantitative real-time PCR. The expressed sequence tag (EST) database (http://www.arabidopsis.org) currently has 31, 23 and 17 cDNA representatives for *ETO1*, *EOL1* and *EOL2*, respectively (as of 10 May 2008), indicating that all three genes are expressed at reasonably similar low levels in Arabidopsis. RNA gel blot analysis of the total RNA showed that *ETO1* and *EOL1* have similar expression patterns in a range of tissues and developmental stages, with the highest levels found in flowers (Figure 7a). Levels of both were near the detection limit in 10-day-old green seedlings, and were not induced upon exposure to 10 μM ACC, as compared with *ERF1*, which is known to be ethylene induced (Solano *et al*., 1998). Transcript levels for *EOL2* were noticeably different from *ETO1* and *EOL1*, and appeared to be more constitutively expressed in green and etiolated seedlings (Figure 7a).

Real-Time PCR analysis qualitatively supported these expression patterns. For example, *ETO1* and *EOL1* displayed similar patterns of transcript abundance, with the highest levels of each being found in flowers, whereas *EOL2* was more constitutively expressed over a broad range of tissues (Figure 7b). The abundance of the *ETO1*, *EOL1* and *EOL2* transcripts was not affected by ACC, indicating that the degradation pathway requiring these BTB proteins is not upregulated by ethylene. Analysis of publicly available microarray databases (Zimmermann *et al*., 2004) also indicated that the abundance of the *ETO1* and *EOL1* transcripts is not substantially altered by various stresses (except by hypoxia, where a greater than twofold decrease was reported for *EOL1*) or exposure to various plant hormones (data not shown). In contrast, transcript levels for *EOL2* did show some significant changes, including a decrease upon treatment of seedlings with hydrogen peroxide (greater than fivefold), infection with *Botrytis cinerea* (greater than twofold), and low potassium and glucose levels (greater than two- and greater than fourfold, respectively). Conversely, several hormones increased *EOL2* mRNA levels, including methyl jasmonate (greater than sixfold), gibberellin (greater than threefold), and auxin and zeatin (greater than fourfold) (data not shown). Taken together, the data suggest that expression of *EOL2* is controlled by a number of factors, whereas the expression of *ETO1* and *EOL1* are under more developmental control, and are less affected by the external environment.

Discussion

Prior studies have implicated the BTB proteins EOL1 and EOL2, along with ETO1, in the proteolytic control of type-2 ACSs, through the direct interaction of the BTB proteins with the C-terminal ends of the ACSs (Chae *et al*., 2003; Wang *et al*., 2004; Yoshida *et al*., 2005). Here, we provide further support for this mode of action by showing that EOL1 and EOL2 contribute to the control of the ethylene-associated phenotype of etiolated seedlings, ethylene biosynthesis and the accumulation of a type-2 ACS (ACS5) protein through the analysis of single, double and triple mutant combinations, affecting *ETO1*, *EOL1* and *EOL2*. Whereas homozygous *eol1−1*, *eol2−2* and *eol1−1 eol2−2* plants are phenotypically indistinguishable from the wild type when grown in the dark or in the light, the triple mutant combination with *eto1−13* displays a stronger ethylene overproduction phenotype in etiolated plants, produces significantly more ethylene and accumulates more of Myc-ACS5 reporter, compared with the *eto1−13* single mutant. Like ETO1, EOL1 specifically interacts via Y2H with the Arabidopsis type-2 ACSs ACS4, ACS5 and ACS9, and not with members of the type-1 (ACS2 and ACS6) and type-3

(ACS7), clades. This interaction is largely abolished by removal of the C-terminal domain of ACS5, or by C-terminal mutations known to stabilize ACS5 and ACS9 *in planta*.

Collectively, the data indicate that the corresponding BTB^{EOL1} and BTB^{EOL2} complexes play a minor role in controlling ethylene synthesis in etiolated seedlings, which only becomes apparent phenotypically upon elimination of the BTB^{ETO1} complex. This accentuated phenotype is best seen upon the addition of the ACS inhibitor AVG, where substantially higher concentrations of the inhibitor were needed to reverse the triple response phenotype. This phenotype was caused by the increased ethylene production resulting from a stronger stabilization of type-2 ACSs, as is shown by the enhanced accumulation of the Myc-ACS5 protein in these mutant backgrounds. Homozygous *eto1−13 eol1−1 eol2−2* seedlings treated with AVG to suppress endogenous ethylene synthesis responded normally to exogenous ethylene, and could be phenotypically rescued by the ethylene receptor antagonist silver, indicating that the enhanced phenotype was related to ethylene biosynthesis, and that aspects of ethylene perception or general growth were not altered upon loss of these BTB proteins.

Our Y2H binding studies with ETO1 and EOL1 agree with prior data showing that the interactions of ETO1-type proteins involve the recognition of a conserved sequence close to the C terminus of type-2 ACSs. More specifically, Yoshida *et al*. (2006) have proposed, through interaction studies with the tomato *Le*ETO1 ortholog of Arabidopsis ETO1, and the type-2 ACS *Le*ACS3, that the signature 'target of ETO1' or TOE motif, bearing a near invariant WVFRLSF/W sequence, is the site that directly interacts with the TPR repeats of the ETO1 proteins. When appended to a type-1 ACS (*Le*ACS2) or GFP, the TOE motif appeared to induce instability *in planta*, strongly suggesting that it can work in the absence of other sequences to target ACSs for degradation.

The abundance of type-1 ACSs may be similarly regulated by C-terminal recognition followed by ubiquitination, but it remains unclear which E3(s) are responsible. For type-1 ACSs, such as Arabidopsis ACS6, it appears that phosphorylation by an MAPK cascade involving MPK6 is a key regulatory step that prevents recognition by the UPS, thus stabilizing the protein (Joo *et al*., 2008; Liu and Zhang, 2004). The site of phosphorylation has been tentatively mapped to a collection of serines near the C terminus of ACS6, thus providing a simple model where the introduction of negative charges near the E3-recognition site abrogates E3 binding (Joo *et al*., 2008). A similar mechanism has been proposed for regulating type-2 ACS recognition by the BTB^{ETO1} E3, but for these ACSs, a CDPK has been implicated in the phosphorylation step (Hernandez Sebastia *et al*., 2004). A possible CDPK phosphorylation site near the C terminus of type-2 ACSs includes a serine that could serve as the phosphate acceptor. However, our data showing that the introduction of alanine, or the phosphomimic aspartic acid, does not detectably affect the Y2H interaction of ETO1 or EOL1 with ACS5, argues that this residue is either not the phosphorylation site or, if modified, that this phosphoserine is not the sole determinant in blocking the interaction of type-2 ACSs with BTB E3s containing ETO1, EOL1 or EOL2.

Phylogenetic studies performed by us and others have identified ETO1-type sequences in numerous plant species, including the fern *Ceratopteris richardii* (one gene) and the mosses *Physcomitrella patens* (two genes) and *Selaginella moellendorfi* (two genes), but not in the green algae *Chlamydomonas reinhardtii* and *Ostreococcus lucimarinus*. We also detected two genes encoding potential ACS orthologs in *P. patens*, although their classification into type-1, −2 or −3 clades was ambiguous. Thus, it is possible that the proteolytic control of ACSs by BTB E3s arose early in land-plant evolution (Gingerich *et al*., 2007; Yoshida *et al*., 2006; MJC and DJG, unpublished data). Furthermore, the presence of multiple ETO1-related proteins in plants, ranging from bryophytes to dicots and moncots, suggests that the collective control of ACSs by multiple BTB proteins is common within the plant kingdom.

The question then arises why plants need additional BTB proteins like EOL1 and EOL2, if, in Arabidopsis, ETO1 by itself appears to suffice in controlling type-2 ACS levels (at least phenotypically)? Differential expression patterns could explain part of this redundancy. Although the EST database revealed that *ETO1*, *EOL1* and *EOL2* are all expressed at similar levels, RNA-gel blot analysis, real-time PCR and DNA microarray studies indicate that *EOL2* and the *ETO1/EOL1* pair are differentially expressed, with *EOL2* being more responsive to hormones and several environmental stresses. In some situations such as infection with *B. cinerea*, the drop in *EOL2* mRNAs could in turn help increase ethylene synthesis, by slowing the degradation of the target type-2 ACSs. Transcript levels for *ETO1*, *EOL1* and *EOL2* are not significantly upregulated by ethylene, implying that the synthesis of these BTB proteins is not induced by ethylene in an effort to dampen ethylene production by a negative feedback loop.

A second possibility is that each BTB protein is specific for individual type-2 ACS targets. Whereas our Y2H data indicate that both ETO1 and EOL1 can interact with members of the type-2 clade, we noticed that the *eto3* mutation in ACS9 differentially attenuated binding. Whereas the binding of $ACS9^{eto3}$ to EOL1 was only partially compromised, as compared with $ACS9^{WT}$, its interaction with ETO1 was strongly blocked, suggesting that ETO1 and EOL1 have different affinities for the ACS9 isoform. Clearly, more interaction studies will be needed to confirm this possibility. A third possibility is that EOL1 and EOL2 play important roles during specific ethylene responses, not studied in detail here. Although we have examined the mutant combinations throughout their life cycle in search of additional phenotypic defects, it remains possible that we missed more subtle ethylene-related processes selectively controlled by EOL1 and EOL2.

Our studies with ETO1, EOL1 and EOL2 provide another example for the importance of ubiquitination in plants, and the combinatorial exploitation of specific E3s in target recognition. Prior studies with Arabidopsis have shown that the TIR1/AFB1−5 family (Parry and Estelle, 2006), EBF1 and EBF2 (Gagne *et al*., 2004; Guo and Ecker, 2003; Potuschak *et al*., 2003), and SNEEZY and SLEEPY F-box proteins (Dill *et al*., 2004; Strader *et al*., 2004) assemble several SCF E3 isoforms that work collectively to ubiquitinate the cognate families of target AUX/IAA, EIN3/EIL1 and Della proteins, as mechanisms to regulate auxin, ethylene and gibberellin signaling, respectively. Some of the TIR1/ABF1–ABF5 family may have differential affinities for their targets (Parry and Estelle, 2006), whereas EBF1 and EBF2 appear to work in temporally distinct manners (Binder *et al*., 2007). As with ETO1, these mechanisms of regulation are apparent in more ancient land plants, indicating that the complex use of ubiquitination for developmental control appeared early in plant evolution. Such complexity in turn may help explain the extremely large numbers of E3s that possibly exist in plants, and suggests that the combinatorial use of E3s to direct the turnover of families of key targets is common to the plant kingdom (Smalle and Vierstra, 2004). For the ethylene system alone, the UPS in general, and individual E3s in particular, have now been implicated in controlling the levels of the ethylene receptors, EIN3/EIL1, and type-1 and type-2 ACSs, with additional targets likely to be found in the future (e.g. type-3 ACSs, ERFs and ACOs; see above and Chen *et al*., 2007), indicating that proteolysis plays a pivotal role in regulating signaling by this hormone.

Experimental procedures

Yeast two-hybrid (Y2H) analysis

Arabidopsis type-1 (*ACS2* and *ACS6*), type-2 (*ACS4*, *ACS5* and *ACS9*) and type-3 (*ACS7*) *ACSs* (Yoshida *et al*., 2005), and *ETO1*, *EOL1* and *EOL2*, cDNAs were cloned into the pEG202-GW bait or pJG4-S-GW prey plasmids, respectively (Gyuris *et al*., 1993; Holt *et al*., 2005), and were then transformed into the yeast strain pSH18−34 by the LiCl method (Gyuris

et al., 1993). Three independent transformants for each assay were then analyzed for interactions using the β-galactosidase assay, in combination with the substrate *O*-nitrophenyl-β-galactoside (ONPG; Clontech Laboratories, http://www.clontech.com). Each colony was grown overnight in 1 ml of non-induction liquid drop-out medium (–histidine/uracil/tryptophan; MP Biomedicals, http://www.mpbio.com) at 28°C, diluted to an OD_{600} of 0.2 in 3 ml of inductive drop-out medium (2% galactose, 1% raffinose, –histidine/uracil/tryptophan), and were then grown overnight. The culture was concentrated into 1 ml of 100 mM sodium phosphate (pH 7.0), 10 mM KCl, 1 mM $MgSO_4$, and then 4 mg ml^{-1} ONPG was added. After 50 min, the reaction was stopped by the addition of 1 M Na_2CO_3, and the absorbance of the culture was measured at 420 nm, and then standardized for cell number by OD_{600}. The Y2H data represent the average of three separate experiments, with the omission of four spurious data points.

Mutant construction and plant growth conditions

The *eto1−13*, *eol1−1* and *eol2−2* T-DNA insertion mutants in the *Arabidopsis thaliana* Col-0 background were as described by Gingerich *et al*. (2005). Combinatorial mutants were created by genetic crosses. Homozygous lines were identified in the F_2 generation by PCR-based genotyping with appropriate primer combinations (Gingerich *et al*., 2005). Primers included the left border T-DNA sequence (Lba1, TGGTTCACGTAGTGGGCCATCG), forward and reverse primers for *ETO1* (#1 TGAGCCATCTTCTCAACCAAATCA and #2 AAAAAGATACCACAAACAAACACA), forward and reverse primers for *EOL1* (#3 CAAGCCAAAACCAAAGTGGACA and #4 CTCGAGAAGGCAACCGAATTG), and forward and reverse primers for *EOL2* (#5 TGTTGAGTGCCAACATTGCCT and #6 TCTCTTGCTCTCTCCGTCTCCC) (see Figure 2). The *eto1−13 eol1−1 eol2−2* mutant was constructed by crossing *eol1−1 eol2−2* (male) with *eol1−1 eto1−13* (female). Dark-grown seedlings in the F_2 generation predicted to overproduce ethylene by their *ctr1*-like phenotype were genotyped to identify homozygous triple mutants.

Growth assays

For hypocotyl growth assays, surface-sterilized seeds were planted on half-strength MS medium minus sucrose, either with or without various concentrations of $AgNO_3$, AVG or ACC, and were stratified for 4 days in the dark at 4°C. Seeds were exposed to 1−2 h of white light before being transferred to the dark for 3 days at 22°C. Each treatment data point represents the average (±SE) of at least 30 seedlings. For ethylene treatments, seedlings were grown in a continuous gas flow-through system, in which the flow rate was regulated to maintain the various ethylene concentrations. For analysis of adult plants, plants were transferred from the agar plates to soil, and were then exposed to a long-day photoperiod (16-h light/8-h dark).

Hypocotyl elongation kinetics on etiolated seedlings were as described by Binder *et al*. (2004b). Surface-sterilized seeds were planted on half-strength solid MS medium (pH 5.7) containing 10 μM AVG, but no added sucrose, were stratified for 2−4 days at 4°C, and were then exposed to white light for 2−4 h prior to placing the plates vertically in the dark for 2 days at 22°C. Once the germinating seedlings reached a height of 2−4 mm, growth rates were measured using images captured from either an EDC-1000N CCD camera (Electrim Corp., http://www.electrim.com) or an Infinity 2−1M digital camera (Luminera Corporation, http://www.lumenera.com), in conjunction with light provided by an infrared light-emitting diode. Growth rates were calculated using custom software generated by Dr Edgar Spalding in LABVIEW 5.0 (National Instruments, http://www.ni.com), as previously described (Folta and Spalding, 2001). Average growth rates were calculated using at least four seedlings from a minimum of three separate experiments.

Ethylene production measurements

Surface-sterilized seeds (40−80 seeds) were germinated in 22-ml gas chromatography vials on 0.4% agar containing 3 ml of full-strength MS medium plus 1% sucrose. Following a five-day stratification at 4°C, the seeds were exposed to white light for 4−6 h. The vials were capped, incubated at 22°C for 4 days in the dark, and were then frozen to −20°C. The accumulated ethylene in the vials was measured by gas chromatography, as described in Vogel *et al*. (1998). Ethylene concentrations were measured three times for each of three replicate vials. Ethylene production was then calculated by dividing the ethylene concentration by the number of seedlings in the vial.

RNA gel blot analysis

Total RNA was extracted from various tissues using the Mini-POP method. Briefly, tissue was ground at liquid nitrogen temperatures, and then homogenized in 1 ml per ~ 400 mg fresh weight of RNA extraction buffer (100 mM Tris-HCl, pH 8.0, 20 mM LiCl, 100 mM Na_4EDTA, 100 nM 2-mercapthoethanol, 16.8 mg ml^{-1} aurintricarboxylic acid; Sigma, http://www.sigmaaldrich.com). After phenol/chloroform extraction, RNA was precipitated with 3 M LiCl, resuspended in water, and then re-precipitated with ethanol. RNA (10 μg) was electrophoresed in 1% agarose gels, and then blotted and baked onto Hybond-XL nylon membranes (Amersham Biosciences, http://www.amersham.com). Methylene blue staining was performed to assure uniform loading and transfer. The membranes were probed with ^{32}P-labeled RNA produced using the SP6/T7 Riboprobe™ system (Promega, http://www.promega.com), as described in Smalle *et al*. (2002). cDNA probes for *ETO1*, *EOL1* and *EOL2* (500−700 bp) were generated by RT-PCR of Arabidopsis RNA using the primers: *ETO1* (GGGACAGACCTCCTTTTGGT and CCTGCCACAACAATCCATAG), *EOL1* (GGTCTAGCTCGTGTCCATTTCC and GGCTATTAACACGGCTATGG) and *EOL2* (TGCCAACATTGCCTCAATAG and GGTAGCCCTCGAATGATGAA). These products were then cloned into the pGEMTeasy vector (Promega).

Real-Time PCR

Total RNA was extracted from various tissues using the RNeasy plant kit (Qiagen, http://www.qiagen.com), treated with 1 μg of DNase (RQ1 DNase; Promega), and was then converted to cDNA using Superscript II (Invitrogen, http://www.invitrogen.com). The cDNA was treated with Rnase H and precipitated with 50% isopropanol. The cDNA at a dilution of 1:625 was subjected to real-time PCR using the iCycler (Bio-Rad, http://www.bio-rad.com) with iQ Supermix (Bio-Rad), in combination with gene-specific primers for *ETO1*, *EOL1*, *EOL2*, *ERF1* and *PP2A-1* (*At1g59830*, the gene encoding protein phosphatase 2A-1). *PP2A-1* was used as the sample template because this transcript is evenly expressed throughout the tissues tested (Czechowski *et al*., 2005). The PCR products were confirmed as correct by agarose gel electrophoresis of the samples, followed by ethidium bromide staining. The relative expression level for each gene was calculated using the Delta–Delta cycle threshold (C_t) method (Wong and Medrano, 2005), using *PP2A-1* as the control. The expression levels were standardized to 10-day-old seedlings grown in air (1.0, relative expression) for each gene. Primers used for amplification included: *ETO1* (GGTCTTGCACGTGTTTATCACCTG and GTGGTCGTCCATAAGAACTGCGG), EOL1 (GTGCACACCAAGGTCTAGCTCGTG and CCGACTATCCATCAACACTGCGGC), *EOL2* (GTGAGGAGATGACAAAGCTGATCGAGAAG and GATCATCCATCAGCACGGCAGCT), *ERF1* (CAGTCCCCATTCTCCGGCTTCTC and GATCGGAAGGTCTTGACTATCCGAGTC) and *PP2A-1* (GTTCCACACGAAGGACCAATGTGC and CACTGTCACTACGTTCTTTTCCTGACACC).

Immunoblot analysis of Myc-ACS5 protein

The triple mutant *eto1−13 eol1−1 eol2−2* was crossed with a Col-0 transgenic plant containing the Dex-inducible *MYC-ACS5* transgene system, previously described by Chae *et al*. (2003). F_2 plants hemizygous for the transgene (+/− *MYC-ACS5*), and homozygous for either wild type or single, double or triple mutant combinations of *eol1−1, eol2−2* or *eto1−13* were identified and allowed to self cross. Approximately 100 seedlings of the progeny (segregating 1:2:1 for the *MYC-ACS5* transgene) were collected and rapidly frozen after growth for 3 days in the dark on half-strength MS medium, supplemented with 12 nM Dex (Sigma-Aldrich). Total protein was isolated by homogenization in 2 μL per seedling of SDS sample buffer (125 mM Tris-HCl, pH 6.8, 4% SDS, 20% glycerol and 10% 2-mercaptoethanol), and was then clarified by centrifugation at 10 000 ***g***. The extracts were subjected to SDS-PAGE and immunoblot analysis with anti-Myc antibodies (Roche, http://www.roche.com) and anti-PBA1 antibodies (Smalle *et al*., 2002).

RT-PCR of the MYC-ACS5 *transcript*

Total RNA was extracted using the RNeasy Plant Kit (Qiagen) from 100 3-day-old etiolated seedlings segregating for the *MYC-ACS5* transgene. After treatmeant with RQ1 DNase (Promega), 2 μg of the RNA was used for cDNA synthesis in conjunction with an oligo $dT_{(18)}$ primer for first-strand synthesis, and the Superscript II RT enzyme (Invitrogen). Semi-quantitative RT-PCR was performed with this template using ExTaq Polymerase (Takara, http://www.takara-bio.com). The *MYC-ACS5* mRNA transcript was amplified using a 5′ primer ending at the *ATG* initiation codon for *ACS5* (TGAATTCGGTACCCCGGGAAATG), in combination with a 3′ primer within the *ACS5* coding region (GTGCCTGAATAGATCTCGTCGCTAATG). The control *UBC21* mRNA was amplified using primers TCATCCTTTCTTAGGCATAGCGGC and TTAGAGATGCAGGCATCAACAGCG.

Acknowledgments

We thank Joseph Walker, Melissa Wei, and Dr. Donald Salter for technical help. This research was supported by grants from the National Science Foundation to R.D.V.

(Arabidopsis 2010 Program – MCB-0115870) and J.J.K. (MCB-0541973), and a National Institute of Heath postdoctoral fellowship to D.J.G. (F32-GM68361).

References

Abeles, FB.; Morgan, PW.; Saltveit, MEJ. Ethylene in Plant Biology. Vol. 1. Academic Press; New York: 1992.

Alonso JM, Hirayama T, Roman G, Nourizadeh S, Ecker JR. EIN2, a bifunctional transducer of ethylene and stress responses in Arabidopsis. Science 1999;284:2148–2152. [PubMed: 10381874]

Argueso CT, Hansen M, Kieber JJ. Regulation of ethylene biosynthesis. J. Plant Growth Reg 2007;26:92–105.

Benavente LM, Alonso JM. Molecular mechanisms of ethylene signaling in Arabidopsis. Mol. Biosyst 2006;2:165–173. [PubMed: 16880934]

Binder BM, Mortimore LA, Stepanova AN, Ecker JR, Bleecker AB. Short-term growth responses to ethylene in Arabidopsis seedlings are EIN3/EIL1 independent. Plant Physiol 2004a;136:2921–2927. [PubMed: 15466219]

Binder BM, O'Malley RC, Wang W, Moore JM, Parks BM, Spalding EP, Bleecker AB. Arabidopsis seedling growth response and recovery to ethylene. A kinetic analysis. Plant Physiol 2004b;136:2913–2920. [PubMed: 15466220]

Binder BM, Walker JM, Gagne JM, Emborg TJ, Hemmann G, Bleecker AB, Vierstra RD. The Arabidopsis EIN3 binding F-Box proteins EBF1 and EBF2 have distinct but overlapping roles in ethylene signaling. Plant Cell 2007;19:509–523. [PubMed: 17307926]

Bostick M, Lochhead SR, Honda A, Palmer S, Callis J. Related to ubiquitin 1 and 2 are redundant and essential and regulate vegetative growth, auxin signaling, and ethylene production in Arabidopsis. Plant Cell 2004;16:2418–2432. [PubMed: 15319484]

Chae HS, Faure F, Kieber JJ. The *eto1*, *eto2*, and *eto3* mutations and cytokinin treatment increase ethylene biosynthesis in Arabidopsis by increasing the stability of ACS protein. Plant Cell 2003;15:545–559. [PubMed: 12566591]

Chang C, Kwok SF, Bleecker AB, Meyerowitz EM. *Arabidopsis* ethylene-response gene *ETR1*: similarity of product to two-component regulators. Science 1993;262:539–544. [PubMed: 8211181]

Chao Q, Rothenberg M, Solano R, Roman G, Terzaghi W, Ecker JR. Activation of the ethylene gas response pathway in Arabidopsis by the nuclear protein ETHYLENE-INSENSITIVE3 and related proteins. Cell 1997;89:1133–1144. [PubMed: 9215635]

Chen YF, Shakeel SN, Bowers J, Zhao XC, Etheridge N, Schaller GE. Ligand-induced degradation of the ethylene receptor ETR2 through a proteasome-dependent pathway in Arabidopsis. J. Biol. Chem 2007;282:24752–24758. [PubMed: 17595158]

Christians MJ, Robles LM, Zeller SM, Larsen PB. The *eer*5 mutation, which affects a novel proteasome related subunit, suggests a prominent role for the COP9 signalosome in resetting the ethylene-signaling pathway in Arabidopsis. Plant J 2008;55:467–477. [PubMed: 18429939]

Czechowski T, Stitt M, Altmann T, Udvardi MK, Scheible WR. Genome-wide identification and testing of superior reference genes for transcript normalization in Arabidopsis. Plant Physiol 2005;139:5–17. [PubMed: 16166256]

Dill A, Thomas SG, Hu J, Steber CM, Sun TP. The Arabidopsis F-box protein SLEEPY1 targets gibberellin signaling repressors for gibberellin-induced degradation. Plant Cell 2004;16:1392–1405. [PubMed: 15155881]

Folta KM, Spalding EP. Unexpected roles for cryptochrome 2 and phototropin revealed by high-resolution analysis of blue light-mediated hypocotyl growth inhibition. Plant J 2001;26:471–478. [PubMed: 11439133]

Gagne JM, Smalle J, Gingerich DJ, Walker JM, Yoo SD, Yanagisawa S, Vierstra RD. Arabidopsis EIN3-binding F-box 1 and 2 form ubiquitin-protein ligases that repress ethylene action and promote growth by directing EIN3 degradation. Proc. Natl Acad. Sci. U.S.A 2004;101:6803–6808. [PubMed: 15090654]

Gingerich DJ, Gagne JM, Salter DW, Hellmann H, Estelle M, Ma L, Vierstra RD. Cullins 3a and 3b assemble with members of the Broad Complex/Tramtrack/Bric-a-Brac (BTB) protein family to form essential ubiquitin-protein ligases (E3s) in Arabidopsis. J. Biol. Chem 2005;280:18810–18821. [PubMed: 15749712]

Gingerich DJ, Hanada K, Shiu SH, Vierstra RD. Large-scale, lineage-specific expansion of a Broad Complex/Tramtrack/Bric-a-Brac ubiquitin-ligase gene family in rice. Plant Cell 2007;19:2329–2348. [PubMed: 17720868]

Guo H, Ecker JR. Plant responses to ethylene gas are mediated by SCF(EBF1/EBF2)-dependent proteolysis of EIN3 transcription factor. Cell 2003;115:667–677. [PubMed: 14675532]

Guzman P, Ecker JR. Exploiting the triple response of Arabidopsis to identify ethylene-related mutants. Plant Cell 1990;2:513–523. [PubMed: 2152173]

Gyuris J, Golemis E, Chertkov H, Brent R. Cdi1, a human G1 and S phase protein phosphatase that associates with Cdk2. Cell 1993;75:791–803. [PubMed: 8242750]

Hernandez Sebastia C, Hardin SC, Clouse SD, Kieber JJ, Huber SC. Identification of a new motif for CDPK phosphorylation *in vitro* that suggests ACC synthase may be a CDPK substrate. Arch. Biochem. Biophys 2004;428:81–91. [PubMed: 15234272]

Hirayama T, Kieber JJ, Hirayama N, Kogan M, Guzman P, Nourizadeh S, Alonso JM, Dailey WP, Dancis A, Ecker JR. RESPONSIVE-TO-ANTAGONIST1, a Menkes/Wilson disease-related copper transporter, is required for ethylene signaling in Arabidopsis. Cell 1999;97:383–393. [PubMed: 10319818]

Holt BF, Belkhadir Y, Dangl JL. Antagonistic control of disease resistance protein stability in the plant immune system. Science 2005;309:929–932. [PubMed: 15976272]

Hua J, Chang C, Sun Q, Meyerowitz EM. Ethylene insensitivity conferred by Arabidopsis *ERS* gene. Science 1995;269:1712–1714. [PubMed: 7569898]

Hua J, Sakai H, Nourizadeh S, Chen QG, Bleecker AB, Ecker JR, Meyerowitz EM. *EIN4* and *ERS2* are members of the putative ethylene receptor gene family in Arabidopsis. Plant Cell 1998;10:1321–1332. [PubMed: 9707532]

Johnson PR, Ecker JR. The ethylene gas signal transduction pathway: a molecular perspective. Annu. Rev. Genet 1998;32:227–254. [PubMed: 9928480]

Joo S, Liu Y, Lueth A, Zhang S. MAPK phosphorylation-induced stabilization of ACS6 protein is mediated by the non-catalytic C-terminal domain, which also contains the cis-determinant for rapid degradation by the 26S proteasome pathway. Plant J 2008;54:129–140. [PubMed: 18182027]

Kieber JJ, Rothenberg M, Roman G, Feldmann KA, Ecker JR. CTR1, a negative regulator of the ethylene response pathway in Arabidopsis, encodes a member of the Raf family of protein kinases. Cell 1993;72:427–441. [PubMed: 8431946]

Larsen PB, Cancel JD. A recessive mutation in the RUB1-conjugating enzyme, RCE1, reveals a requirement for RUB modification for control of ethylene biosynthesis and proper induction of basic chitinase and PDF1.2 in Arabidopsis. Plant J 2004;38:626–638. [PubMed: 15125769]

Liang X, Oono Y, Shen NF, Kohler C, Li K, Scolnik PA, Theologis A. Characterization of two members (*ACS1* and *ACS3*) of the 1-*AMINOCYCLOPROPANE-1-CARBOXYLATE SYNTHASE* gene family of *Arabidopsis thaliana*. Gene 1995;167:17–24. [PubMed: 8566772]

Liu Y, Zhang S. Phosphorylation of 1-aminocyclopropane-1-carboxylic acid synthase by MPK6, a stress-responsive mitogen-activated protein kinase, induces ethylene biosynthesis in Arabidopsis. Plant Cell 2004;16:3386–3399. [PubMed: 15539472]

Ortega-Martinez O, Pernas M, Carol RJ, Dolan L. Ethylene modulates stem cell division in the *Arabidopsis thaliana* root. Science 2007;317:507–510. [PubMed: 17656722]

Parry G, Estelle M. Auxin receptors: a new role for F-box proteins. Curr. Opin. Cell Biol 2006;18:152–156. [PubMed: 16488128]

Potuschak T, Lechner E, Parmentier Y, Yanagisawa S, Grava S, Koncz C, Genschik P. EIN3-dependent regulation of plant ethylene hormone signaling by two Arabidopsis F box proteins: EBF1 and EBF2. Cell 2003;115:679–689. [PubMed: 14675533]

Potuschak T, Vansiri A, Binder BM, Lechner E, Vierstra RD, Genschik P. The exoribonuclease XRN4 is a component of the ethylene response pathway in Arabidopsis. Plant Cell 2006;18:3047–3057. [PubMed: 17085683]

Schaller, GE.; Kieber, JJ. Ethylene.. In: Somerville, CR.; Meyerowitz, EM., editors. The Arabidopsis Book. American Society of Plant Biologists; Rockville, MD: 2002. doi/10.1199/tab.0071

Smalle J, Vierstra RD. The ubiquitin 26S proteasome proteolytic pathway. Annu. Rev. Plant Biol 2004;55:555–590. [PubMed: 15377232]

Smalle J, Kurepa J, Yang P, Babiychuk E, Kushnir S, Durski A, Vierstra RD. Cytokinin growth responses in Arabidopsis involve the 26S proteasome subunit RPN12. Plant Cell 2002;14:17–32. [PubMed: 11826296]

Solano R, Stepanova A, Chao Q, Ecker JR. Nuclear events in ethylene signaling: a transcriptional cascade mediated by *ETHYLENE-INSENSITIVE3* and *ETHYLENE-RESPONSE-FACTOR1*. Genes Dev 1998;12:3703–3714. [PubMed: 9851977]

Strader LC, Ritchie S, Soule JD, McGinnis KM, Steber CM. Recessive-interfering mutations in the gibberellin signaling gene *SLEEPY1* are rescued by overexpression of its homologue, *SNEEZY*. Proc. Natl. Acad. Sci. U.S.A 2004;101:12771–12776. [PubMed: 15308775]

Tsuchisaka A, Theologis A. Unique and overlapping expression patterns among the Arabidopsis 1-amino-cyclopropane-1-carboxylate synthase gene family members. Plant Physiol 2004;136:2982–3000. [PubMed: 15466221]

Vogel JP, Woeste KE, Theologis A, Kieber JJ. Recessive and dominant mutations in the ethylene biosynthetic gene *ACS5* of Arabidopsis confer cytokinin insensitivity and ethylene overproduction, respectively. Proc. Natl. Acad. Sci. U.S.A 1998;95:4766–4771. [PubMed: 9539813]

Wang KL, Yoshida H, Lurin C, Ecker JR. Regulation of ethylene gas biosynthesis by the Arabidopsis ETO1 protein. Nature 2004;428:945–950. [PubMed: 15118728]

Wang NN, Shih MC, Li N. The GUS reporter-aided analysis of the promoter activities of Arabidopsis ACC synthase genes *AtACS4*, *AtACS5*, and *AtACS7* induced by hormones and stresses. J. Exp. Bot 2005;56:909–920. [PubMed: 15699063]

Woeste KE, Ye C, Kieber JJ. Two Arabidopsis mutants that overproduce ethylene are affected in the posttranscriptional regulation of 1-aminocyclopropane-1-carboxylic acid synthase. Plant Physiol 1999;119:521–530. [PubMed: 9952448]

Wong ML, Medrano JF. Real-time PCR for mRNA quantitation. BioTechniques 2005;39:1–11.

Yamagami T, Tsuchisaka A, Yamada K, Haddon WF, Harden LA, Theologis A. Biochemical diversity among the 1-amino-cyclopropane-1-carboxylate synthase isozymes encoded by the Arabidopsis gene family. J. Biol. Chem 2003;278:49102–49112. [PubMed: 12968022]

Yanagisawa S, Yoo S-D, Sheen J. Differential regulation of EIN3 stability by glucose and ethylene signalling in plants. Nature 2003;425:521–525. [PubMed: 14523448]

Yoo SD, Cho YH, Tena G, Xiong Y, Sheen J. Dual control of nuclear EIN3 by bifurcate MAPK cascades in C_2H_4 signalling. Nature 2008;451:789–795. [PubMed: 18273012]

Yoshida H, Nagata M, Saito K, Wang KL, Ecker JR. Arabidopsis ETO1 specifically interacts with and negatively regulates type 2 1-aminocyclopropane-1-carboxylate synthases. BMC Plant Biol 2005;5:14. [PubMed: 16091151]

Yoshida H, Wang KL, Chang CM, Mori K, Uchida E, Ecker JR. The ACC synthase TOE sequence is required for interaction with ETO1 family proteins and destabilization of target proteins. Plant Mol. Biol 2006;62:427–437. [PubMed: 16897471]

Zimmermann P, Hirsch-Hoffmann M, Hennig L, Gruissem W. GENEVESTIGATOR. Arabidopsis microarray database and analysis toolbox. Plant Physiol 2004;136:2621–2632. [PubMed: 15375207]

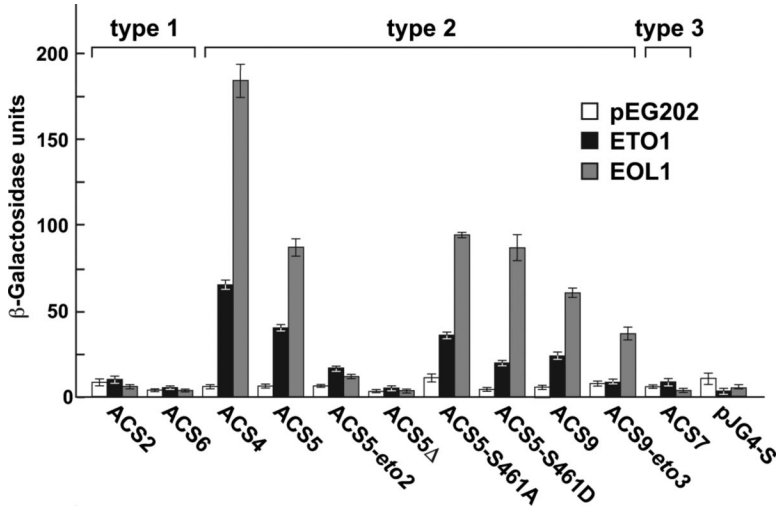

Figure 1.

Arabidopsis ETO1 and EOL1 specifically interact with type-2 1-aminocyclopropane-1-carboxylic acid (ACC) synthases (ACSs) via their C-terminal ends. Full-length ETO1 and EOL1 proteins fused to the GAL4 activation domain in pEG202-GW were tested by yeast two-hybrid (Y2H) screening for interactions with various Arabidopsis type-1 (ACS2 and ACS6), type-2 (ACS4, ACS5 and ASCS9) and type-3 ACSs (ACS7) fused to the GAL4 DNA-binding domain in pJG4-S-GW. Yeasts containing empty pJG4-S-GW and pEG202-GW vectors were included as controls. ACS5-*eto2* contains an insertion that disrupts the primary sequence, beginning at the last 12 amino acids in ACS5, ACS5-S461A and ACS5-S461D contain alanine and aspartic acid substitutions of Ser-461, and ACS5Δ is also missing the 78 C-terminal amino acids. ACS9-*eto3* contains a V456N substitution. The strength of the binding was measured by βgalactosidase activity.

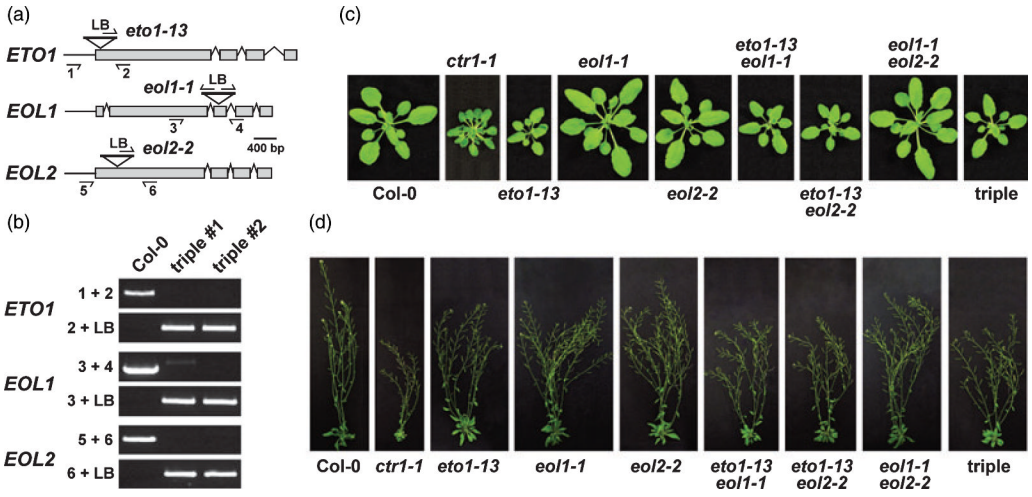

Figure 2.

Phenotypic analysis of light-grown combinatorial mutants affecting *ETO1*, *EOL1* and *EOL2*.

(a) Diagrams of the genes, positions of the T-DNA insertions, and locations of primers used in PCR-based genotyping. The exons are shown in boxes, with the introns shown by lines; LB, left border primer.

(b) Confirmation of the homozygous *eto1−13 eol1−1 eol2−2* plants by genomic PCR. DNA was isolated from wild-type (WT) and triple-mutant seedlings, and was then subjected to PCR with the primer pairs shown in panel (a).

(c and d) Representative plants homozygous for the various mutations grown in long days (16-h light/8-h dark), for either 4 weeks (c) or six weeks (d). Homozygous *ctr1−1* plants are included for comparison.

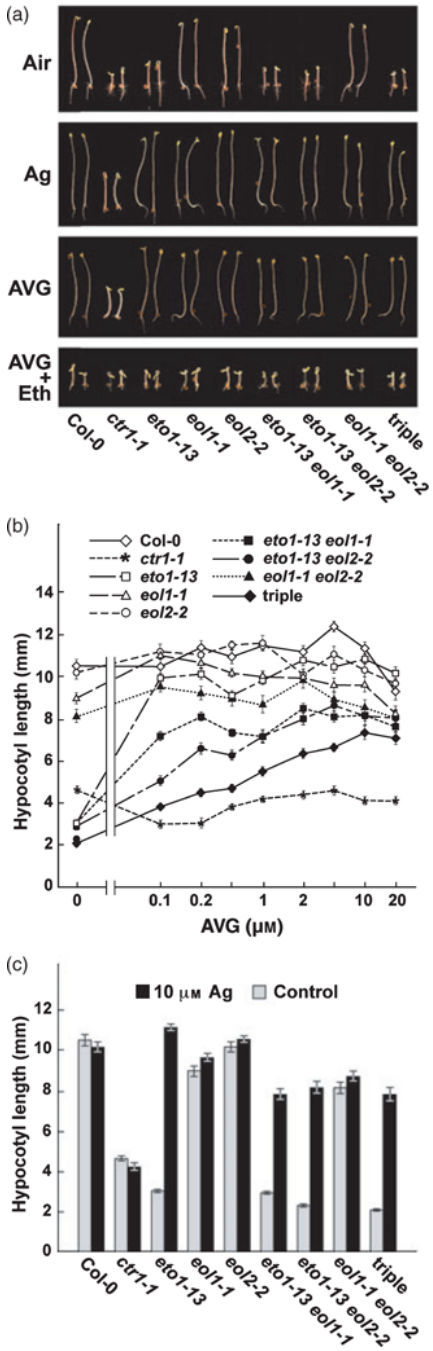

Figure 3.

Hypocotyl lengths of combinatorial mutants affecting *ETO1, EOL1* and *EOL2* in response to ethylene, silver and aminoethoxyvinylglycine (AVG).

(a) Representative 3-day-old etiolated seedlings grown in air, 10 μM silver (Ag), 10 μM AVG and 10 μM AVG plus 100 μL L^{-1} ethylene. Two representative seedlings are shown per line.

(b) Hypocotyl elongation in response to various concentrations of AVG.

(c) Hypocotyl elongation in response to 10 μM silver (Ag). Each point/bar represents the average height (± SE) of at least 30 seedlings. Homozygous *ctr1−1* seedlings are included for comparison.

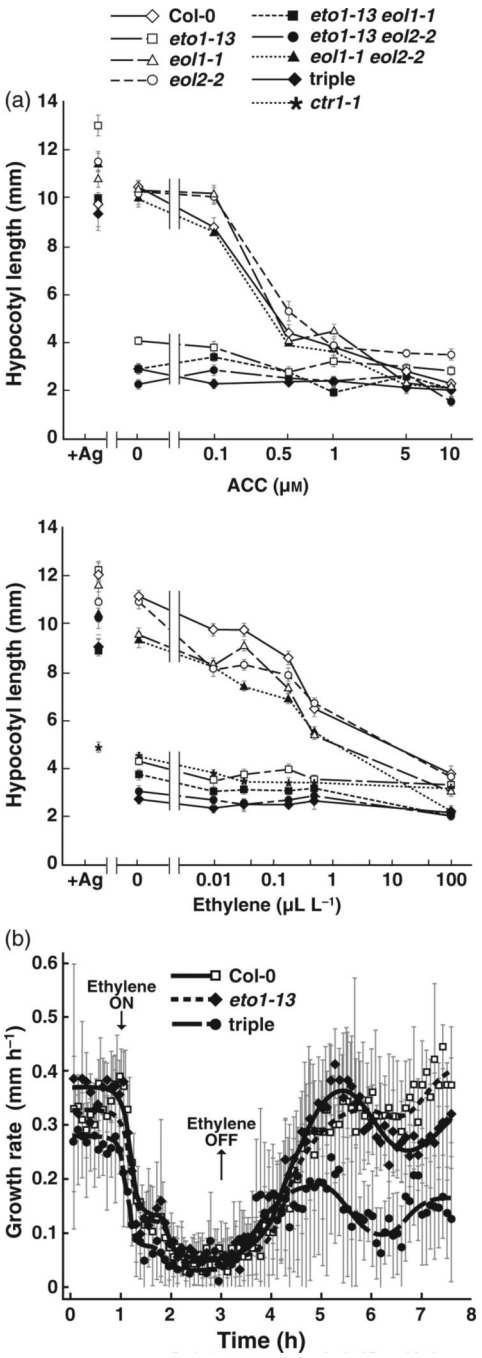

Figure 4.

Hypocotyl growth of combinatorial mutants affecting *ETO1*, *EOL1* and *EOL2*.

(a) Hypocotyl elongation in response to 1-aminocyclopropane-1-carboxylic acid (ACC; top panel) and ethylene (bottom panel). Three-day-old etiolated seedlings were grown in various concentrations of ACC or ethylene. Seedlings grown on 10 μM silver (Ag) and *ctr1−1* seedlings are included for comparisons.

(b) Elongation kinetics of 3-day-old hypocotyls in response to ethylene plus 10 μM AVG. Elongation rates were recorded for 1 h in air, followed by a 2-h exposure to 10 μL L^{-1} ethylene, and then followed by 4.5 h of recovery in air.

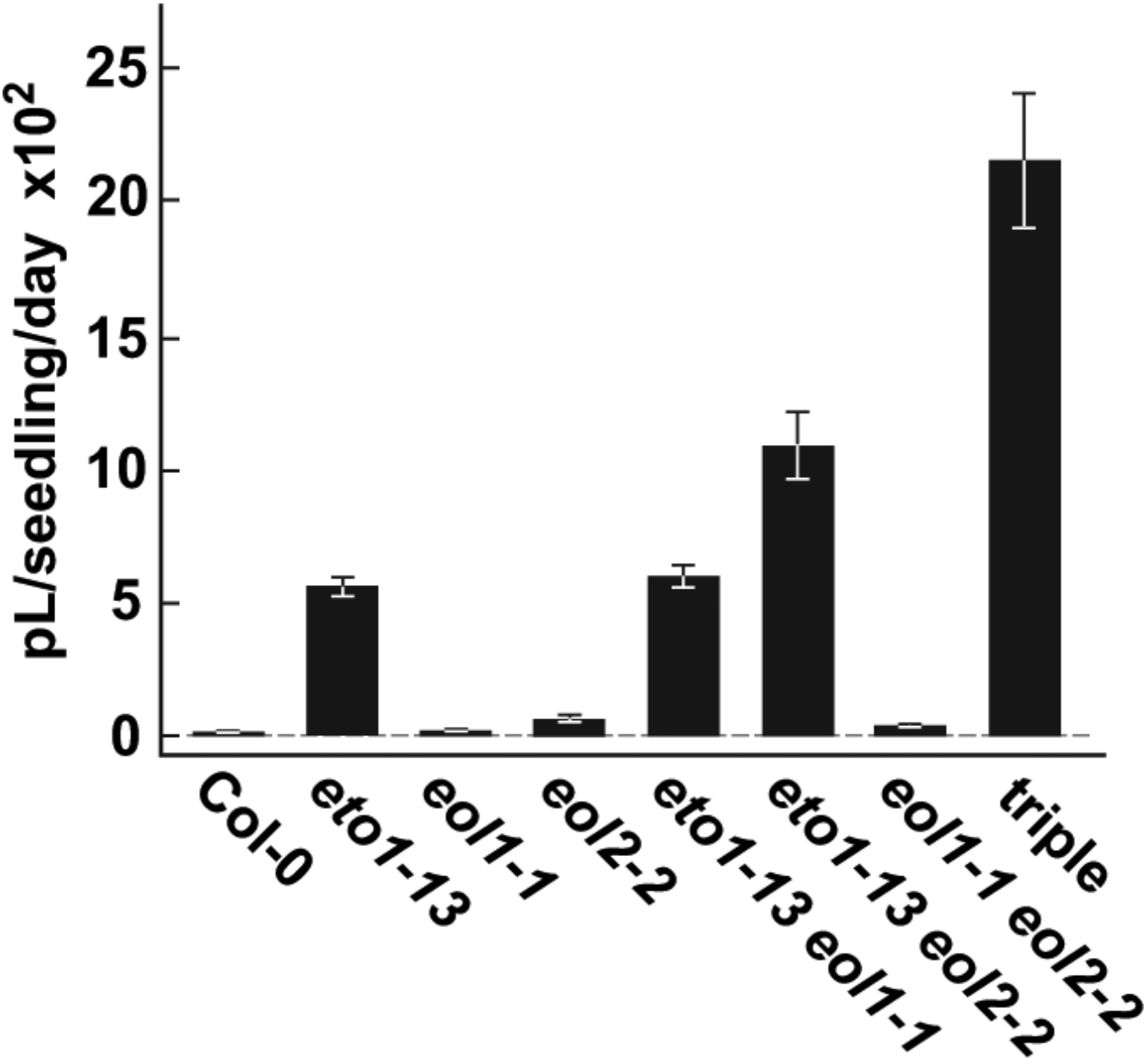

Figure 5.
Ethylene emission from combinatorial mutants affecting *ETO1*, *EOL1* and *EOL2*. Etiolated seedlings were grown in sealed vials, and the volume of ethylene released was quantified by gas chromatography. Each bar represents the average (± SE) of three separate vials, with each vial measured in triplicate.

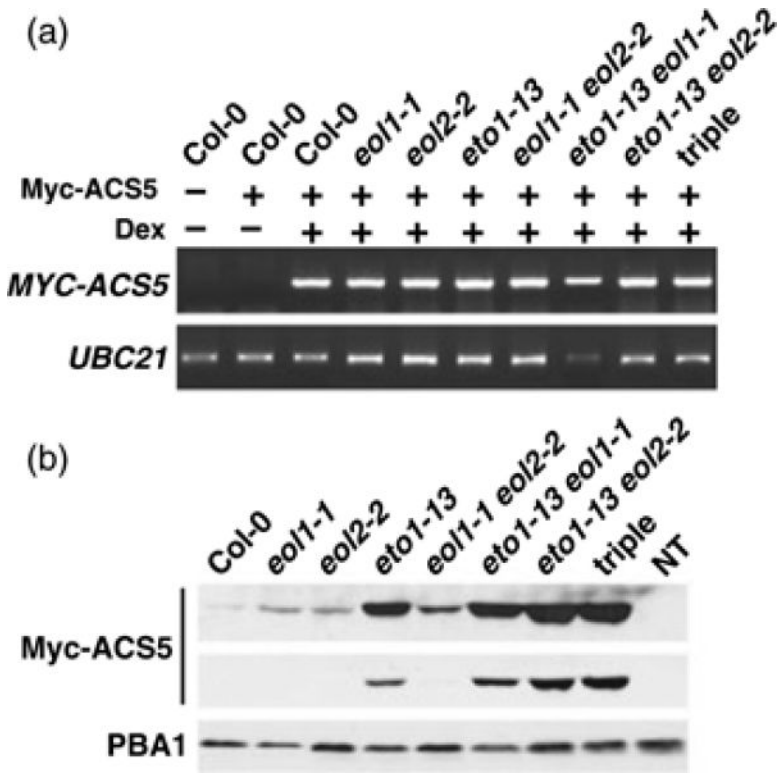

Figure 6.

Steady-state levels of ACS5 increase in combinatorial mutants affecting *ETO1, EOL1* and *EOL2*. A Dex-inducible transgene expressing Myc-ACS5 was introgressed into the homozygous mutant backgrounds, and the seedlings were grown on medium with or without 12 nM Dex.

(a) RT-PCR analysis of total RNA, demonstrating expression of *MYC-ACS5* in the presence of Dex. *UBC21* was used to confirm that near-equivalent quantities of template cDNA were added to each PCR reaction.

(b) Steady-state abundance of Myc-ACS5 protein. Crude extracts of plants exposed to Dex were subjected to immunoblot analysis with anti-Myc antibodies. A longer (top panel) and shorter exposure (bottom panel) of the same blot are shown. Anti-PBA1 antibodies were used to confirm the near-equal loading of the samples; NT, a non-transformed plant missing the *MYC-ACS5* transgene.

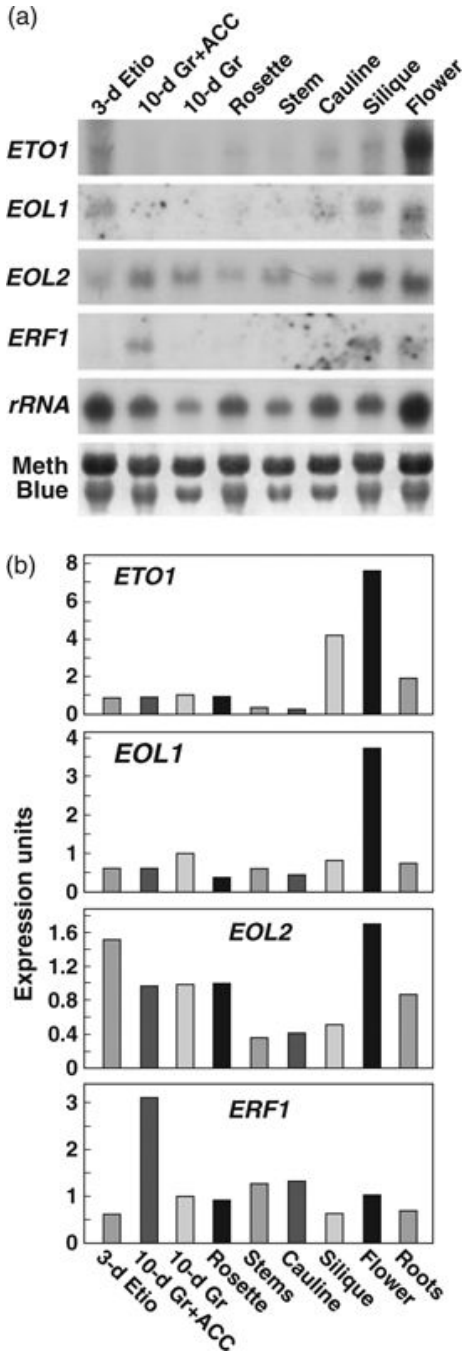

Figure 7.

Expression profiles of the *ETO1*, *EOL1* and *EOL2* mRNAs.

(a) RNA gel blot analysis of total RNA isolated from various Arabidopsis organs. Total RNA (10 μg) was loaded in each lane. 18 S rRNA is shown as a loading control. Ten-day-old green seedlings were exposed to 10 μ_M ACC for 3 days prior to harvest.

(b) Relative abundance of *ETO1*, *EOL1* and *EOL2* mRNAs in various organs from Arabidopsis, as measured by real-time PCR. The bars represent the average of three PCR reactions, and were normalized relative to those obtained with RNA samples from seedlings grown for 10 days in air; Etio, etiolated seedlings; Gr, green seedlings.